Volume 58(2): 183–193, 2010
Journal of Histochemistry & Cytochemistry
http://www.jhc.org

ARTICLE

The Actin-binding Protein Caldesmon Is in Spleen and Lymph Nodes Predominately Expressed by Smooth-muscle Cells, Reticular Cells, and Follicular Dendritic Cells

Christoph N. Köhler

Institute II of Anatomy, Medical Faculty, University of Cologne, Cologne, Germany

SUMMARY Reticular cells and follicular dendritic cells (FDCs) build up a framework that underlies the compartmentalization of spleens and lymph nodes. Subpopulations of reticular cells express the smooth-muscle isoform of actin, indicative of a specialized contractile apparatus. We have investigated the distribution of the actin-binding protein caldesmon in spleen and lymph nodes of mice and rats. Caldesmon modulates contraction and regulates cell motility. Alternative splicing of transcripts from a single gene results in high-molecular-mass isoforms (*h*-caldesmon) that are predominately expressed by smooth-muscle cells (SMCs), and low-molecular-mass isoforms (*l*-caldesmon) that are thought to be widely distributed in non-muscle tissues, but the distribution of caldesmon in spleen and lymph nodes has not been reported. We have performed Western blot analysis and immunohistochemistry using four different antibodies against caldesmon, among these a newly developed polyclonal antibody directed against recombinant mouse caldesmon. Western blot analysis showed the preponderance of *l*-caldesmon in spleen and lymph nodes. Our results from immunohistochemistry demonstrate caldesmon in SMCs, as expected, but also in reticular cells and FDCs, and suggest that the isoform highly expressed by reticular cells is *l*-caldesmon. In spleen of SCID mice, caldesmon was expressed by reticular cells in the absence of lymphocytes. **(J Histochem Cytochem 58:183–193, 2010)**

KEY WORDS
blood vessels
cytoskeleton
spleen
lymph nodes
lymphatic tissue
smooth muscle

Spleens and lymph nodes display a compartmentalized structure that is based on a skeleton built up by reticular cells in red pulp, marginal zone, and periarteriolar lymphatic sheet (PALS) and by follicular dendritic cells (FDCs) in follicles and germinal centers. This structural organization directs lymphocyte traffic and interaction as well as antigen and chemokine flow (Veerman and van Ewijk 1975; Nolte et al. 2003; Bajénoff et al. 2006; for review see Balogh et al. 2008; Lokmic et al. 2008). FDCs in germinal centers trap and retain immune complexes and promote affinity maturation of B-cells (Aydar et al. 2005). The reticular network must permit great volume changes during an immune response, e.g., associated with the development and regression of germinal centers (Veerman and Vries 1976; Liu et al. 1991; Hollowood and Macartney 1992). Accordingly, contractile proteins characteristic of smooth muscle are expressed by reticular cells (Pinkus et al. 1986; Toccanier-Pelte et al. 1987; Satoh et al. 1997,2009; Steiniger et al. 2001).

Caldesmon is a thin filament-associated actin-, myosin-, tropomyosin-, and calmodulin-binding protein (for review see Sobue and Sellers 1991; Huber 1997; Dabrowska et al. 2004; Wang 2008). Low-molecular-mass isoforms of caldesmon (*l*-caldesmon, 70 to 80 kDa) are thought to be widely distributed in non-muscle tissues, but only a few studies have used immunohistochemistry to investigate the distribution of caldesmon in selected tissues (Ban et al. 1984; Fujita et al. 1984; Ishimura et al. 1984). *l*-Caldesmon has a

Correspondence to: Christoph N. Köhler, Institute II of Anatomy, Medical Faculty, University of Cologne, Joseph Stelzmann Straße 9, 50931 Cologne, Germany. E-mail: c.koehler@uni-koeln.de

Received for publication July 15, 2009; accepted October 8, 2009 [DOI: 10.1369/jhc.2009.954651].

role in the organization and stabilization of the microfilament network, thus regulating proliferation and migration (Kordowska et al. 2006; Yokouchi et al. 2006; Morita et al. 2007). High-molecular-mass isoforms (*h*-caldesmon, 120 to 150 kDa) are predominantly expressed in differentiated smooth-muscle cells (SMCs), with only a few reported exceptions; platelets, colorectal pericryptal fibroblasts, and myoepithelial cells of galactophorous sinuses of human breast tissue contain *h*-caldesmon as well (Kakiuchi et al. 1983; Frid et al. 1992; Lazard et al. 1993; Nakayama et al. 1999). In vitro studies suggest that *h*-caldesmon modulates the contraction of smooth muscle by inhibiting actomyosin ATPase. The inhibitory effect of *h*-caldesmon on smooth-muscle contraction can be reversed by binding to Ca^{2+}/calmodulin or by phosphorylation of caldesmon (Ngai and Walsh 1984; Horiuchi et al. 1986; Mak et al. 1991; Foster et al. 2000; for review see Arner and Pfitzer 1999; Kim et al. 2008). *h*-Caldesmon has gained importance as a smooth-muscle differentiation marker in tumor diagnosis (Miettinen et al. 1999; Visée et al. 2005), distinguishing myofibroblastic tumors from smooth-muscle tumors (Ceballos et al. 2000; Perez-Montiel et al. 2006; Qiu et al. 2008). Some histopathological studies have also demonstrated the normal distribution of *h*-caldesmon in additional tissues, including the presence of caldesmon in human FDCs from normal and neoplastic lymph follicles (Tsunoda et al. 1999; Mesquita et al. 2009), but which cells express caldesmon in spleen and lymph nodes has not been demonstrated to date.

We have used a newly developed polyclonal antibody against mouse caldesmon, as well as antibodies commercially available, to investigate the expression of caldesmon in spleen and lymph nodes of mice and rats.

Materials and Methods

Animals

Nine female and male C57BL/6 JOlaHsd mice, age 4 to 12 months, were obtained from Harlan (Horst, The Netherlands). Six female and male Wistar rats, age 4 months, were bred in the Institute of Anatomy, Cologne, Germany; three female SCID mice (CB17/Icr-Prkdc scid/Crl), age 8 weeks, were obtained from Charles River Laboratories (Sulzfeld, Germany). The animals were handled according to the guidelines of the animal care committee of the University of Cologne.

Gel Electrophoresis and Immunoblotting

Mouse and rat spleens, lymph nodes, and lungs were washed in Tris-base sodium chloride buffer, pH 7.6 (TBS), frozen in liquid nitrogen, and stored at −80C until use. For gel electrophoresis, tissues were homogenized in lysis buffer [50 mM Tris-base, 0.15 M NaCl, 5 mM EDTA, 1 mM PMSF (Sigma-Aldrich; Taufkirchen, Germany)] and centrifuged at 3000 × g for 20 min at 4C. The supernatant was used, and the amount of protein in the supernatant was determined using the BCA protein assay kit (Perbio; Bonn, Germany). Proteins were separated by 6% SDS-PAGE, electroblotted onto a nitrocellulose membrane, and subsequently immersed in blocking buffer consisting of TBS containing 0.1% Tween 20 (TBST) and 5% non-fat dry milk for 1 hr at room temperature. The membranes were washed with TBS containing 0.1% Tween 20, followed by incubation overnight at 4C with primary antibodies, and diluted in TBST containing 5% non-fat dry milk. After washing in TBST, the blot was incubated with horseradish peroxidase (HRP)-coupled secondary antibodies to rabbit (Dako; Hamburg, Germany) or mouse IgG (Sigma-Aldrich), diluted in TBST containing 5% non-fat dry milk, for 1 hr at room temperature. Finally, the blot was washed again in TBST and developed with chemiluminescent substrate (Roche; Mannheim, Germany).

Tissue Processing

Animals were deeply anesthetized (0.02 g tribromethanol/100 g body weight intraperitoneally for rats; 0.055 g tribromethanol/100 g body weight intraperitoneally for mice), perfused via the left ventricle with 0.1 M PBS, pH 7.4, for 3 min, followed by 4% paraformaldehyde (PFA) or 4% PFA/0.2% picric acid for 15 min. Spleens and lymph nodes were removed, post-fixed in the same fixative at 4C overnight, dehydrated, embedded in paraffin or frozen in isopentane in liquid N_2, and cryoprotected in graded sucrose. Sections 4–7 μm thick were cut and mounted on silane (paraffin sections) or polysine-coated slides (frozen sections). To prepare acetone-fixed frozen sections, organs were removed without prior fixation, frozen in isopentane in liquid N_2, cut, fixed in ice-cold acetone for 10 min, and air-dried for 45 min.

Antibodies

Four different antibodies against caldesmon were used. A rabbit polyclonal antibody was produced in the Institute of Physiology, University of Cologne, by immunization of rabbits with recombinant mouse *h*-caldesmon. *h*-Caldesmon was expressed as a Strep-Tag fusion protein in HEK-EBNA cells. Full-length *h*-caldesmon was injected into rabbits. The caldesmon-specific antibody was purified from rabbit serum by affinity chromatography. It was used at a concentration of 0.23 μg/ml for immunohistochemistry or 0.03 μg/ml for Western blot. A rabbit monoclonal caldesmon antibody was obtained from Abcam (Cambridge, UK). This antibody was raised against an epitope around phosphorylated Ser^{789}, but is, according to the manufacturer, not phospho-specific (www.abcam.com/ab32330). It was used diluted 1:20 for immunohistochemistry or 1:250 for Western blot. A so-called human *l*-caldesmon

monoclonal mouse antibody (clone 8/L-Caldesmon, catalog number 610660) was obtained from BD Transduction Laboratories (Heidelberg, Germany) and used diluted 1:100 for immunohistochemistry or 1:6000 for Western blot. This antibody was raised against a fragment of human *l*-caldesmon corresponding to aa 251–395, a sequence that is, however, present in *l*-caldesmon and *h*-caldesmon. A mouse monoclonal antibody to human uterus smooth-muscle extract (clone h-CD), according to the manufacturer specific for *h*-caldesmon, was obtained from Sigma-Aldrich (catalog number C 4562). It was diluted 1:250 for immunohistochemistry or 1:500 for Western blot. A polyclonal rabbit antibody against aa 36–42 of Aβ42 (catalog number 44-344, Biosource; Nivelles, Belgium) and a mouse monoclonal to human paired helical filaments-tau, clone AT8 (code 90343, Innogenetics; Gent, Belgium), which were not expected to stain structures in normal spleen and lymph node, were used as controls to exclude unspecific Fc-receptor–mediated binding. Other antibodies used were a goat polyclonal to a carboxy-terminal epitope of mouse CD3 (sc-1127, Santa Cruz Biotechnology; Heidelberg, Germany) diluted 1:750, a mouse monoclonal to rat FDCs (clone ED5, catalog number MCA530R, Serotec; Düsseldorf, Germany) diluted 1:2000, a rat monoclonal to mouse FDCs (clone FDC-M1, catalog number 551320, BD Biosciences; Heidelberg, Germany) diluted 1:20, a rat monoclonal to mouse interdigitating dendritic cells (IDCs) (clone MIDC-8, catalog number MCA948, Serotec) diluted 1:15, and a rat monoclonal to mouse reticular fibroblasts (clone ER-TR7, catalog number MCA2402, Serotec) diluted 1:20.

Immunohistochemistry

Immunohistochemistry was performed using the avidin-biotin peroxidase method. Paraffin sections were deparaffinized in xylene, rehydrated, and pretreated by boiling three times for 5 min in citrate buffer (pH 6.0) in a microwave oven. After sections were washed in TBS for 5 min and blocked in 20% FBS + 1% BSA for 45 min, primary antibodies diluted in TBS containing 3% non-fat dry milk were applied, and the sections were incubated overnight at 4C. After another three washes in TBS, they were incubated with the appropriate biotinylated secondary antibody for 30 min at room temperature [anti-rabbit IgG (Dianova; Hamburg, Germany) 1:400, anti-mouse IgG (Dianova) 1:250, anti-rat IgG (Dianova) 1:250, or anti-goat IgG (Linaris; Wertheim-Bettingen, Germany) 1:450]. Sections were again washed and incubated with an avidin-biotinylated HRP complex (ABC Elite Kit; Linaris) for another 30 min. Peroxidase activity was visualized by incubating the sections in a chromogen solution containing DAB intensified by the inclusion of 0.6% ammonium nickel sulfate (Fluka; Buchs, Switzerland) and 0.05% imidazol (Fluka), which resulted in a deep blue-gray reaction product.

Double Staining

For light microscopy, sections were consecutively stained with antibodies against IDCs and caldesmon. IDC staining (antibody MIDC-8) was done as described above. Color reaction was performed with the intensified DAB solution. Before staining for caldesmon, the peroxidase from the previous stain was blocked by incubating the sections in 0.3% H_2O_2 in TBS for 30 min at room temperature. The polyclonal caldesmon primary antibody was followed by a peroxidase-coupled anti-rabbit secondary antibody (1:20; Dianova). A chromogen solution with DAB only produced a brown reaction product, indicating caldesmon immunoreactivity.

Immunofluorescence double labeling was performed with primary antibodies consecutively applied overnight at 4C. Incubation with the first primary antibody (clones h-CD, ED5, FDC-M1, and ER-TR7) was followed by incubation with biotinylated anti-mouse or anti-rat IgG (1:250; Dianova) for 30 min at room temperature and then with AlexaFluor 488–conjugated streptavidin (1:200; MoBiTec, Göttingen, Germany) for another 30 min at room temperature. The second primary antibody (caldesmon polyclonal) was detected with AlexaFluor 546–conjugated anti-rabbit IgG (1:400; MoBiTec). Autofluorescence was quenched by incubating the sections in a solution with 4 mM $CuSO_4$/50 mM ammonium acetate for 30 min before the blocking step with 20% FBS/1% BSA.

Digital Imaging

DAB-stained sections were examined with a BX40 microscope (Olympus; Hamburg, Germany) equipped with a ColorView II digital camera (Olympus Soft Imaging Solutions; Münster, Germany). Confocal laser scanning microscopy was performed with an LSM510 confocal microscope (Zeiss; Jena, Germany). Digital images were processed for contrast and brightness using Picture Publisher 8 (Micrografx) and Adobe Photoshop 5.0. Small tissue damages were retouched without altering the scientific information. Images were arranged in Adobe Photoshop 5.0. Images shown in Figures 5C and 5D are composed of two images taken with ×10 objective lens. These images were processed for evenness of illumination.

Results

Testing of the Antibodies and Immunoblot Analysis of Caldesmon Isoform Expression in Spleen and Lymph Nodes

Caldesmon isoforms appear as proteins of 70 to 80 kDa and 120 to 150 kDa, different from their theoretical molecular mass because of aberrant migration

in SDS-PAGE (Huber 1997). The rabbit polyclonal, rabbit monoclonal calSer^{789}, and mouse monoclonal cal$^{251–395}$ antibodies recognized a band at ~74 kDa in lysates of rat spleens and cervical lymph nodes, and a band at ~72 kDa in lysates of mouse spleens corresponding to the reported molecular mass of *l*-caldesmon. For mouse cervical lymph nodes, clear results were only obtained with the caldesmon polyclonal antibody. A band at 130 kDa, the molecular mass of *h*-caldesmon, was barely detectable (Figure 1). Because *h*-caldesmon and *l*-caldesmon differ only by the lack of a central spacer region in *l*-caldesmon, specificity of the *l*-caldesmon antibody for *l*-caldesmon was unlikely. Indeed, this antibody recognized *h*-caldesmon in, e.g., lung, an organ with a higher relative amount of *h*-caldesmon (not shown) and was therefore used to detect all isoforms. We did not obtain a single band at 130 kDa with the monoclonal antibody against *h*-caldesmon as expected, neither in spleen or lymph node nor in lung, but did obtain a band at ~75 kDa, just above the bands detected by the other antibodies. This antibody labeled multiple bands when the concentration was slightly raised (not shown).

Caldesmon Is Highly Expressed by SMCs, Reticular Cells, and FDCs in Spleen and Lymph Nodes

We have compared PFA-fixed paraffin sections, acetone-, PFA- and PFA/picric acid–fixed frozen sections. Best results were obtained with PFA-fixed and PFA/picric acid–fixed frozen sections with microwave pretreatment. There was only slight staining of nuclei when the cal$^{251–395}$ antibody was replaced by similar concentrated isotype-matched mouse IgG against phosphorylated tau (antibody AT8). There was no staining when the caldesmon polyclonal antibody was replaced by polyclonal rabbit IgG of irrelevant specificity (anti-Aβ42), indicating that binding of the caldesmon antibodies was not Fc-receptor mediated. Immunoreactivity was also absent when the primary antibodies were omitted (not shown).

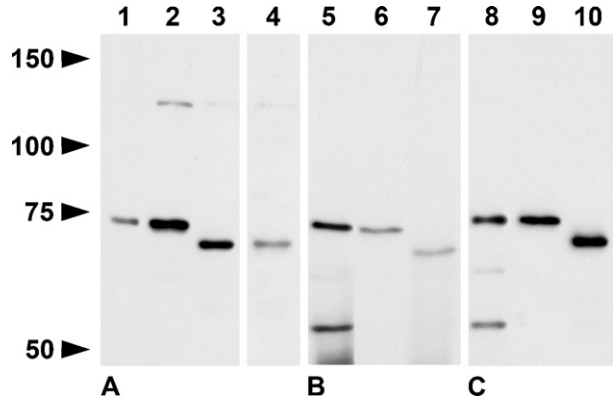

Figure 1 Western blots of rat spleen (Lanes 1, 5, 8), rat lymph node (Lanes 2, 6, 9), mouse spleen (Lanes 3, 7, 10), and mouse lymph node (Lane 4) after 6% SDS-PAGE stained with rabbit polyclonal (**A**, 10 μg per lane loaded), rabbit monoclonal calSe^{789} (**B**, 60 μg per lane loaded), and cal$^{251–395}$ antibodies (**C**, 10 μg per lane loaded). All antibodies recognize a band corresponding to *l*-caldesmon isoforms. A faint band at 130 kDa corresponding to the molecular mass of *h*-caldesmon is also detected in Lanes 2–4. The monoclonal antibodies label an additional band at ~55 kDa in rat spleen, possibly a degradation product or not related to caldesmon (Lanes 5, 8).

We have obtained the same pattern of staining with spleens and lymph nodes from rats and mice. Immunoreactivity of the spleen with the antibody against *h*-caldesmon (clone h-CD) was confined to SMCs in the walls of larger blood vessels and in trabecula (Figures 2A–2C). In addition to the anticipated immunoreactivity of SMCs, the reticular network of the spleen was strongly immunoreactive, with all three antibodies recognizing *l*- and *h*-caldesmon isoforms. Comparably large reticular cells of the PALS displayed a strong immunoreaction (Figures 2D and 2E). Immunoreactivity of IDCs was excluded by double labeling (Figure 2F). A fine mesh of stained cells extended into the marginal zone and red pulp. The caldesmon-positive network overlapped with the ER-TR7 antigen, an extracellular matrix component secreted by reticular cells and incorporated into reticular fibers, which are enwrapped by reticular cell cytoplasm (Figures 3A–3C) (Katakai et al. 2004; Lokmic et al. 2008). There was prominent staining at the marginal sinus surrounding the follicles, similar to the location of MAdCAM-1–positive cells in the murine spleen (Figures 3D, 4A, and 4C) (Tanaka et al. 1996). In the red pulp, large immunoreactive cells with the morphology of megakaryocytes were conspicuous (Figure 2G), in agreement with the known presence of caldesmon in platelets. In line with this, there was punctuate immunoreactivity between clusters of erythrocytes in sinus (not shown). Consistent with immunoreactivity of FDCs, we observed a weakly stained reticular pattern of B-cell follicles that was often stronger in the center of the follicle when polyclonal and cal$^{251–395}$ antibodies were used. However, we obtained only a little staining of the center of follicles with the calSer^{789} antibody (Figure 2E). Immunofluorescence double labeling of the caldesmon-positive reticulum in follicles with FDC-M1, a marker for mouse FDCs (Kosco et al. 1992), confirmed that caldesmon is expressed by FDCs (Figures 3D–3F). Caldesmon-positive cells were also seen in the capsule. The presence of *l*-caldesmon in isolated T-lymphocytes from mouse spleen was demonstrated previously by immunoblotting (Mizushima et al. 1987). We observed only weak immunostaining of lymphocytes of unclear significance just above background levels when frozen sections were used, most pronounced with the caldesmon polyclonal antibody.

Homozygous SCID mice lack functional B- and T-lymphocytes because of an inability to arrange antigen receptor genes (Schuler et al. 1986). Therefore,

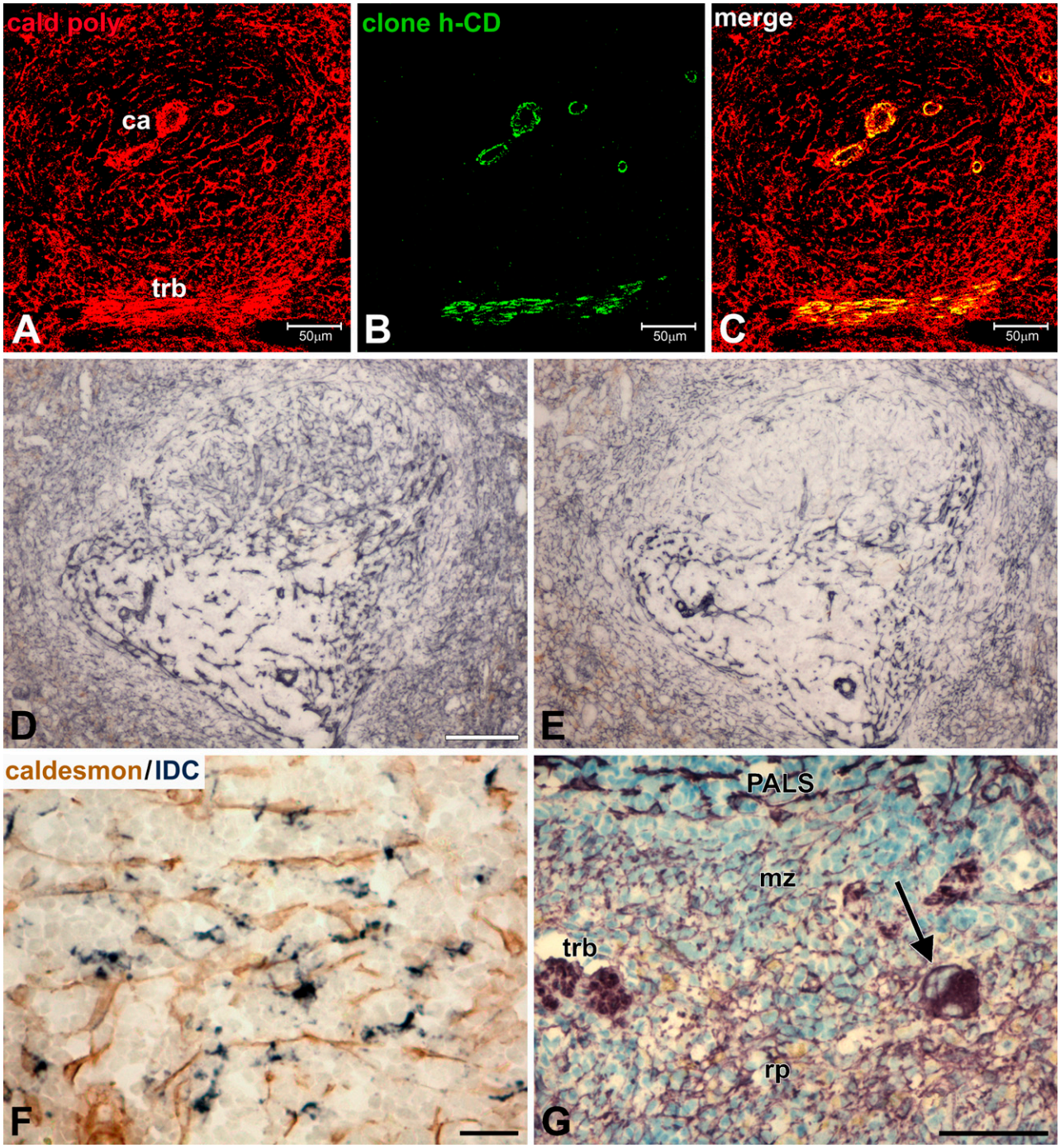

Figure 2 (**A–E**) Seven-μm thick, 4% PFA/0.2% picric acid–fixed, frozen sections of normal rat spleen. (**A–C**) Confocal image (1-μm optical thickness) showing that immunoreactivity with clone h-CD is confined to the wall of a central artery (ca) and trabecula (trb), whereas the caldesmon polyclonal antibody stains these structures also, but in addition, a widespread mesh of elongated cells. (**D,E**) DAB stain with caldesmon polyclonal (**D**) or calSer^{789} (**E**) antibodies of consecutive sections. Caldesmon is expressed by relatively large elongated cells concentrically arranged around the central artery in the periarteriolar lymphatic sheet (PALS) and by smooth-muscle cells of the central artery. A fine network of immunoreactive cells extends into follicles, marginal zone, and red pulp. There is only a little immunoreactivity with the calSer^{789} antibody in the center of the follicle (**E**). (**F,G**) Seven-μm-thick, 4% PFA-fixed, frozen sections of a normal mouse spleen stained brown with the caldesmon polyclonal antibody and deep blue-gray for interdigitating dendritic cells (IDCs) (**F**) or stained with the caldesmon polyclonal antibody and counterstained with Giemsa-solution (**G**). (**F**) Caldesmon-positive reticular cells and IDCs have different morphologies; IDCs seem to adhere to caldesmon-positive reticular cells. (**G**) In the red pulp, a megakaryocyte (arrow) displays strong caldesmon immunoreactivity (deep purple). Trabecula (trb) and the reticular network in PALS, marginal zone (mz) and red pulp (rp) are also stained. Brown, endogenous pigment in macrophages. Bars: **A–C,G** = 50 μm; **D,E** = 100 μm; **F** = 20 μm.

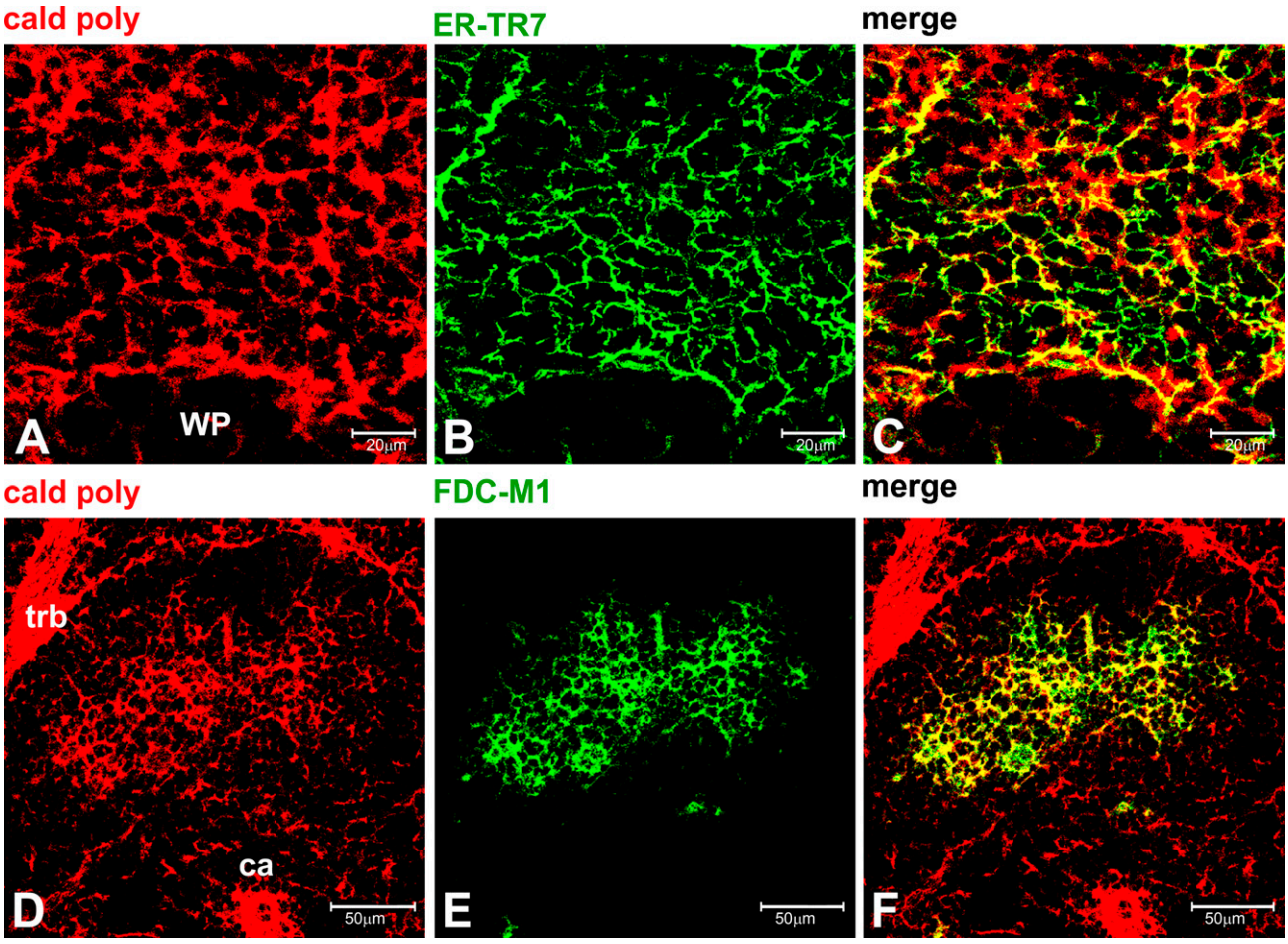

Figure 3 (**A–F**) Ten-μm-thick, acetone-fixed, frozen sections of normal mouse spleen. (**A–C**) Confocal microscopy (0.5-μm optical thickness) showing the colocalization of the fibroblastic reticular cell–derived matrix and caldesmon in the marginal zone. (**D–F**) Confocal microscopy of a follicle (1-μm optical thickness) showing the colocalization of caldesmon and the mouse follicular dendritic cell (FDC) marker FDC-M1 in a well-developed reticulum. WP, white pulp; ca, central artery; trb, trabecula. Bars: **A–C** = 20 μm; **D–F** = 50 μm.

malpighian follicles of SCID spleens consist mainly of loose connective tissue containing a reticulin network, histiocytes, and fibroblasts (Custer et al. 1985). Reticular cells of SCID mice displayed a reduced antigenic diversity, which reappeared after reconstitution with lymphocytes (Yoshida et al. 1993). We have stained spleen sections for caldesmon to examine whether the (near complete) absence of lymphocytes within the reticular mesh of the white pulp would also influence the expression of caldesmon by reticular cells. The malpighian follicles of SCID spleens were smaller, compared with normal spleens, and displayed a dense network of caldesmon-positive reticular cells due to the lack of intervening lymphocytes (Figures 4A–4F).

In cervical and mesenteric lymph nodes, too, the reticular network was strongly immunostained with caldesmon antibodies recognizing *l*- and *h*-caldesmon isoforms in addition to SMCs, similar to the spleen. *h*-Caldesmon immunoreactivity was confined to the wall of a few blood vessels (not shown). Caldesmon-positive elongated cells were located in the capsule, underneath the subcapsular sinus, surrounding sinus and high endothelial venules, and in the medullary cords (Figures 5A–5C). As in spleen, there was also a strong reticular staining pattern in the center of several B-cell follicles with polyclonal (Figure 5A) and $cal^{251–395}$ antibodies (not shown), but not with the $calSer^{789}$ antibody (Figure 5B). Immunofluorescence double labeling for caldesmon and FDC-M1 or ED5, a marker for rat FDCs (Jeurissen and Dijkstra 1986) (not shown), confirmed that FDCs in lymph nodes were immunoreactive for caldesmon. Consecutive DAB-stained sections of normal rat cervical and mesenteric lymph nodes showed a good correspondence in the presence of ED5- and caldesmon-positive reticula in follicles (Figures 5C and 5D).

Discussion

The specificity of the immunolabeling for caldesmon has been confirmed by the use of four different poly-

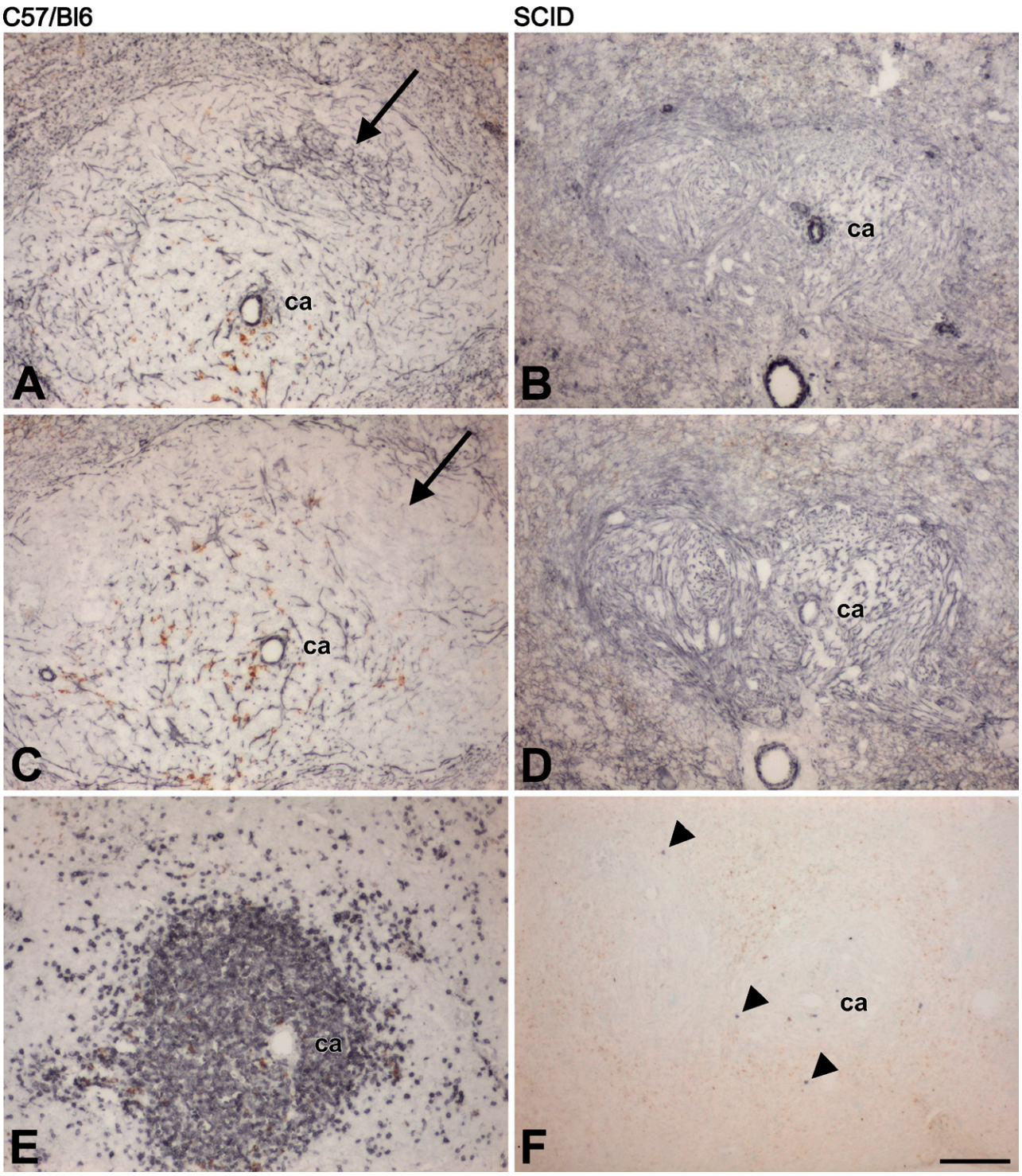

Figure 4 Consecutive frozen sections, 4% PFA–fixed, of spleens from C57/BL6 (**A,C,E**) and SCID mice (**B,D,F**) stained with caldesmon polyclonal (**A,B**), calSer^{789} (**C,D**), and CD3 (**E,F**) antibodies. Only a few T-lymphocytes (arrowheads) can be detected in the SCID spleen (**F**), but reticular cells of SCID mice express caldesmon (**B,D**). (**A,C**) As in rats, there is only a little immunoreactivity in the center of follicles of C57/BL6 mice with the calSe^{789} antibody (arrow in **C**), in contrast to the clearly stained reticulum obtained with the polyclonal antibody (arrow in **A**). ca, central artery; brown color, endogenous pigment. Images shown are representative of results obtained from three different mice per strain. Bar = 200 μm.

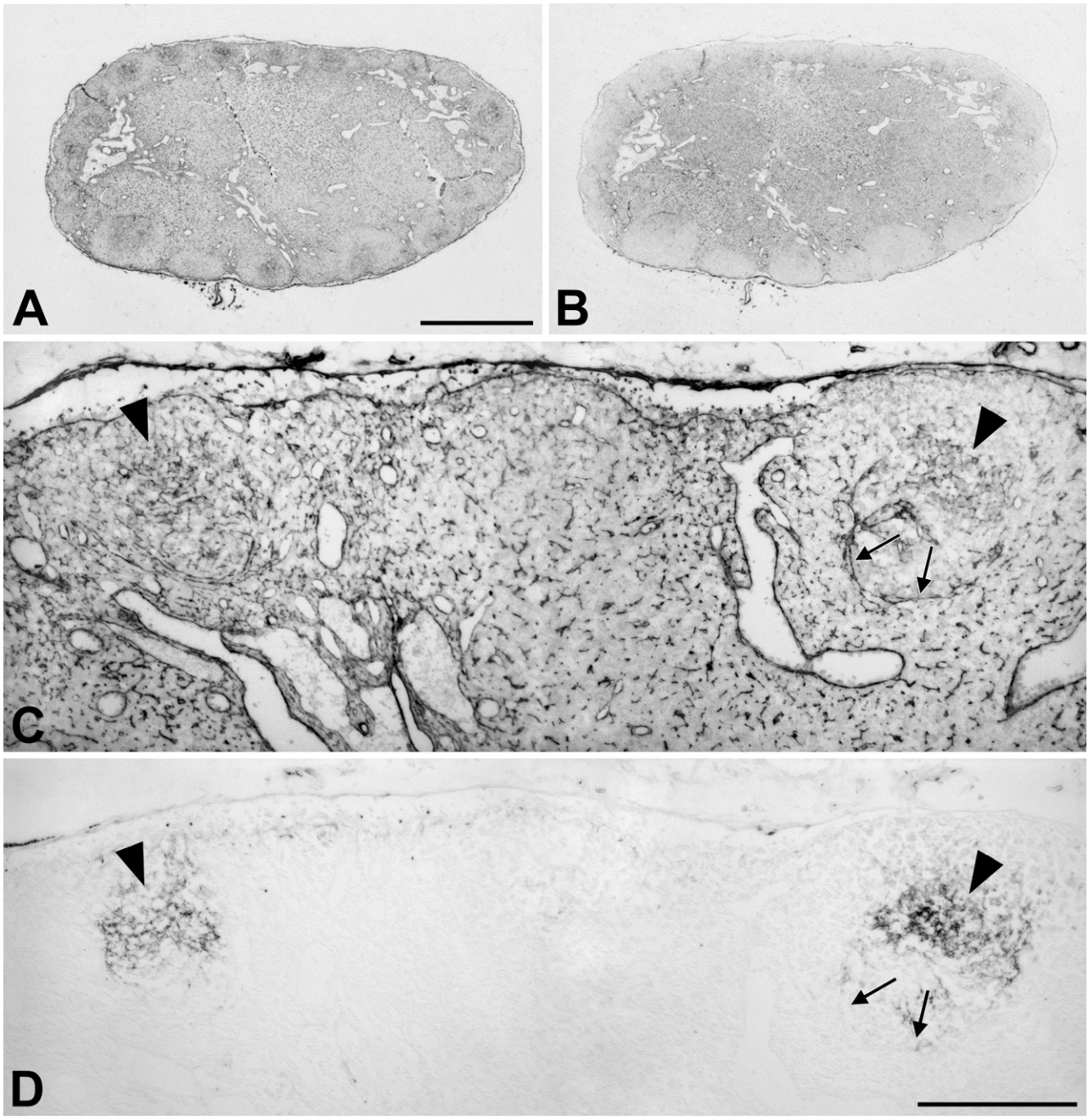

Figure 5 (**A,B**) Seven-μm-thick, 4% PFA/0.2% picric acid–fixed consecutive frozen sections of a normal rat mesenteric lymph node stained with caldesmon polyclonal (**A**) or calSer^{789} (**B**) antibodies shown at low magnification. The capsule, a large blood vessel, the deep cortex, and the medullary cords are immunoreactive. Follicles display stronger caldesmon immunoreactivity in the center (**A**); as in spleen, there is only minimal caldesmon immunoreactivity in the center of follicles with the calSer^{789} antibody (**B**). (**C,D**) Four-μm-thick, 4% PFA/0.2% picric acid–fixed, consecutive frozen sections of a normal rat mesenteric lymph node stained with the caldesmon polyclonal antibody (**C**) and for FDC (**D**), showing the colocalization of immunoreactive reticula (arrowheads) in the light zone of follicles. The deep cortex can be distinguished by the presence of large caldesmon-positive reticulum cells. The border between the deep cortex and the right follicle is indicated by arrows. Some small, round cells located mainly in the subcapsular sinus stain unspecifically because of their content of endogenous peroxidase. Bars: **A,B** = 1 mm; **C,D** = 200 μm.

clonal and monoclonal antibodies against the same protein, recognizing different epitopes and produced in different species. The rabbit polyclonal, rabbit monoclonal calSer^{789}, and mouse monoclonal cal$^{251–395}$ antibodies stained the same bands corresponding to low-molecular-mass isoforms, whereas the high-molecular-mass isoform was barely detectable. This shows the preponderance of *l*-caldesmon in spleen

and lymph nodes. Other investigators have obtained a faint band at 77 kDa and a stronger band at 150 kDa, or only a faint band just below 80 kDa for rat spleen (Sobue et al. 1985; Dingus et al. 1986). Our results also demonstrate that the molecular mass of *l*-caldesmon in spleens and lymph nodes of mice is lower than in rats. Western blots of various cell lines stained for caldesmon showed bands with molecular mass ranging from 71 to 77 kDa (Bretscher and Lynch 1985), indicating, together with our results, tissue- and species-specific variation of the molecular mass of *l*-caldesmon.

The reticular meshwork of all compartments of spleen and lymph nodes was immunoreactive with the three antibodies recognizing *l*- and *h*-caldesmon isoforms, suggesting that a high level of expression of caldesmon is common to virtually all types of reticular cells, including those in the red pulp and FDCs. In contrast, reticular cells of the spleen display an enzyme and an antigenic heterogeneity demonstrated by the use of different antibodies identifying subsets of fibroblastic reticular cells in mouse and rat (Müller-Hermelink et al. 1974; Van den Berg et al. 1989; Yoshida et al. 1991; see Table 3 in Balogh et al. 2004 for overview). Several antibodies distinguish between reticular cells of T- and B-cell areas, suggesting that the antigenic diversity may depend upon the contact with lymphocytes. Experiments with SCID mice showed an influence of B-cells (Yoshida et al. 1993). The widespread distribution of caldesmon and the expression in SCID mice suggest that the regulation of the expression of caldesmon is independent from lymphocytes.

In addition to SMCs, a higher content of caldesmon may be expected in other types of cells also containing a specialized contractile apparatus. At ultrastructural examination, reticulum cells display bundles of microfilaments (Pinkus et al. 1986; Satoh et al. 1997). A subpopulation of reticulum cells expresses the smooth-muscle isoform of actin (α-SMA). In fibroblasts, the expression of α-SMA depends on the extracellular matrix and mechanical stress (Hinz et al. 2007). In human and rat lymph nodes, α-SMA is expressed in parafollicular areas and in the deep cortex by cells with long cytoplasmic extensions (Toccanier-Pelte et al. 1987). In the human spleen, α-SMA is expressed by reticular cells bordering the white pulp and extending mesh-like into the marginal zone. In human and rat spleen, α-SMA–containing reticular cells were also demonstrated in the PALS; but in follicles, these cells were rare, corresponding to sparse reticulum cells and reticulin fibers in this area. FDCs may replace α-SMA–positive reticular cells in germinal centers (Toccanier-Pelte et al. 1987; Satoh et al. 1997,2009; Steiniger et al. 2001). In vivo imaging has shown that the FDC network displays a marked mobility, and FDCs in culture express α-SMA (Bajénoff et al. 2006; Muñoz-Fernández et al. 2006). Another contractile protein, SMC myosin, has a similar distribution in spleen and may also be present in a reticular pattern in follicles of lymph nodes (Pinkus et al. 1986; but see Toccanier-Pelte et al. 1987). When the distribution of α-SMA and SMC myosin is compared with the pattern of high expression of caldesmon in spleen and lymph nodes, expression of caldesmon is more widespread, corresponding better to the mesenchymal origin of cells.

As reported for human FDCs, we have found that rat and mouse FDCs express caldesmon. An obvious difference between the pattern of staining obtained with caldesmon polyclonal and $cal^{251–395}$ antibodies and the results obtained with the $calSer^{789}$ antibody is the lack of a more strongly stained reticulum in the center of follicles with the latter. This could be due either to the fact that the $calSer^{789}$ antibody is less sensitive or to the fact that it is more selective. The inability to stain FDCs seems to be absolute, because other cells were comparably stained. The monoclonal $calSe^{789}$ antibody is directed against an epitope at the extreme C terminus of caldesmon, close to the strong actin-binding domain. It is possible that this epitope is not sufficiently accessible in FDCs.

According to the known distribution of caldesmon isoforms, detection of *h*-caldesmon using clone h-CD was confined to SMCs in trabecula and in the wall of larger blood vessels, suggesting that caldesmon detected in reticular cells is the *l*-caldesmon isoform. This would be consonant with histopathological studies, which demonstrate that myofibroblasts express α-SMA but not *h*-caldesmon (Ceballos et al. 2000; Perez-Montiel et al. 2006; Qiu et al. 2008). The relative proportions of *l*-caldesmon and *h*-caldesmon we have found in Western blot with antibodies recognizing both isoforms would be consistent with the expression of *h*-caldesmon by SMCs only. Thus, spleen and lymph nodes may contain a large population of strongly *l*-caldesmon–positive cells. *l*-Caldesmon in lymphocytes may contribute to the *l*-caldesmon band detected in Western blot as well (Mizushima et al. 1987), but the amount of caldesmon may not be high enough to produce a clear immunohistochemical signal. However, because we could not demonstrate the specificity of the *h*-caldesmon antibody in Western blot, these conclusions remain somewhat uncertain. On the other hand, clone h-CD has been used in many histopathological studies as a marker for SMC-derived tumors, and staining of normal tissues with this antibody has been confined to SMCs and a few other cell types.

In conclusion, based on our immunohistochemical data, caldesmon is, in addition to SMCs, also highly expressed by reticular cells and FDCs in spleen and lymph nodes. The high amount of caldesmon in α-SMA–containing reticular cells may reflect an important role in the regulation of relaxation and contraction of these cells, especially during an immune response.

Acknowledgments

The author wishes to thank Professor G. Pfitzer (Institute of Physiology, University of Cologne) for providing the caldesmon polyclonal antibody. The excellent technical assistance of M. Dinekov is gratefully acknowledged.

Literature Cited

Arner A, Pfitzer G (1999) Regulation of cross-bridge cycling by Ca2+ in smooth muscle. Rev Physiol Biochem Pharmacol 134:63–146

Aydar Y, Sukumar S, Szakal AK, Tew JG (2005) The influence of immune complex-bearing follicular dendritic cells on the IgM response, Ig class switching, and production of high affinity IgG. J Immunol 174:5358–5366

Bajénoff M, Egen JG, Koo LY, Laugier JP, Brau F, Glaichenhaus N, Germain RN (2006) Stromal cell networks regulate lymphocyte entry, migration, and territoriality in lymph nodes. Immunity 25:989–1001

Balogh P, Fisi V, Szakal AK (2008) Fibroblastic reticular cells of the peripheral lymphoid organs: unique features of a ubiquitous cell type. Mol Immunol 46:1–7

Balogh P, Horvath G, Szakal AK (2004) Immunoarchitecture of distinct reticular fibroblastic domains in the white pulp of mouse spleen. J Histochem Cytochem 52:1287–1298

Ban T, Ishimura K, Fujita H, Sobue K, Kakiuchi S (1984) Immunocytochemical demonstration for caldesmon and actin in the striated and smooth muscle cells and non-muscular cells of various organs of rats. Acta Histochem Cytochem 17:331–338

Bretscher A, Lynch W (1985) Identification and localization of immunoreactive forms of caldesmon in smooth and nonmuscle cells: a comparison with the distributions of tropomyosin and alpha-actinin. J Cell Biol 100:1656–1663

Ceballos KM, Nielsen GP, Selig MK, O'Connell JX (2000) Is anti-h-caldesmon useful for distinguishing smooth muscle and myofibroblastic tumors? An immunohistochemical study. Am J Clin Pathol 114:746–753

Custer RP, Bosma GC, Bosma MJ (1985) Severe combined immunodeficiency (SCID) in the mouse. Pathology, reconstitution, neoplasms. Am J Pathol 120:464–477

Dabrowska R, Kulikova N, Gagola M (2004) Nonmuscle caldesmon: its distribution and involvement in various cellular processes. Protoplasma 224:1–13

Dingus J, Hwo S, Bryan J (1986) Identification by monoclonal antibodies and characterization of human platelet caldesmon. J Cell Biol 102:1748–1757

Foster DB, Shen LH, Kelly J, Thibault P, Van Eyk JE, Mak AS (2000) Phosphorylation of caldesmon by p21-activated kinase. Implications for the Ca(2+) sensitivity of smooth muscle contraction. J Biol Chem 275:1959–1965

Frid MG, Shekhonin BV, Koteliansky VE, Glukhova MA (1992) Phenotypic changes of human smooth muscle cells during development: late expression of heavy caldesmon and calponin. Dev Biol 153:185–193

Fujita H, Ishimura K, Ban T, Kurosumi M, Sobue K, Kakiuchi S (1984) Immunocytochemical demonstration of caldesmon and actin in thyroid glands of rats. Cell Tissue Res 237:375–377

Hinz B, Phan SH, Thannickal VJ, Galli A, Bochaton-Piallat ML, Gabbiani G (2007) The myofibroblast: one function, multiple origins. Am J Pathol 170:1807–1816

Hollowood K, Macartney J (1992) Cell kinetics of the germinal center reaction: a stathmokinetic study. Eur J Immunol 22:261–266

Horiuchi KY, Miyata H, Chacko S (1986) Modulation of smooth muscle actomyosin ATPase by thin filament associated proteins. Biochem Biophys Res Commun 136:962–968

Huber PA (1997) Caldesmon. Int J Biochem Cell Biol 29:1047–1051

Ishimura K, Fujita H, Ban T, Matsuda H, Sobue K, Kakiuchi S (1984) Immunocytochemical demonstration of caldesmon (a calmodulin-binding, F-actin-interacting protein) in smooth muscle fibers and absorptive epithelial cells in the small intestine of the rat. Cell Tissue Res 235:207–209

Jeurissen SH, Dijkstra CD (1986) Characteristics and functional aspects of nonlymphoid cells in rat germinal centers, recognized by two monoclonal antibodies ED5 and ED6. Eur J Immunol 16:562–568

Kakiuchi R, Inui M, Morimoto K, Kanda K, Sobue K, Kakiuchi S (1983) Caldesmon, a calmodulin-binding, F actin-interacting protein, is present in aorta, uterus and platelets. FEBS Lett 154: 351–356

Katakai T, Hara T, Sugai M, Gonda H, Shimizu A (2004) Lymph node fibroblastic reticular cells construct the stromal reticulum via contact with lymphocytes. J Exp Med 20:783–795

Kim HR, Appel S, Vetterkind S, Gangopadhyay SS, Morgan KG (2008) Smooth muscle signalling pathways in health and disease. J Cell Mol Med 12:2165–2180

Kordowska J, Huang R, Wang CL (2006) Phosphorylation of caldesmon during smooth muscle contraction and cell migration or proliferation. J Biomed Sci 13:159–172

Kosco MH, Pflugfelder E, Gray D (1992) Follicular dendritic cell-dependent adhesion and proliferation of B cells in vitro. J Immunol 148:2331–2339

Lazard D, Sastre X, Frid MG, Glukhova MA, Thiery JP, Koteliansky VE (1993) Expression of smooth muscle-specific proteins in myoepithelium and stromal myofibroblasts of normal and malignant human breast tissue. Proc Natl Acad Sci USA 90:999–1003

Liu YJ, Zhang J, Lane PJ, Chan EY, MacLennan IC (1991) Sites of specific B cell activation in primary and secondary responses to T cell-dependent and T cell-independent antigens. Eur J Immunol 21:2951–2962

Lokmic Z, Lämmermann T, Sixt M, Cardell S, Hallmann R, Sorokin L (2008) The extracellular matrix of the spleen as a potential organizer of immune cell compartments. Semin Immunol 20:4–13

Mak AS, Watson MH, Litwin CM, Wang JH (1991) Phosphorylation of caldesmon by cdc2 kinase. J Biol Chem 266:6678–6681

Mesquita RA, de Araújo VC, Paes RA, Nunes FD, de Souza SC (2009) Immunohistochemical analysis for CD21, CD35, Caldesmon and S100 protein on dendritic cells types in oral lymphomas. J Appl Oral Sci 17:248–253

Miettinen MM, Sarlomo-Rikala M, Kovatich AJ, Lasota J (1999) Calponin and h-caldesmon in soft tissue tumors: consistent h-caldesmon immunoreactivity in gastrointestinal stromal tumors indicates traits of smooth muscle differentiation. Mod Pathol 12:756–762

Mizushima Y, Kanda K, Hamaoka T, Fujiwara H, Sobue K (1987) Redistribution of caldesmon and tropomyosin associated with concanavalin A receptor capping on splenic T-lymphocytes. Biomed Res 8:73–78

Morita T, Mayanagi T, Yoshio T, Sobue K (2007) Changes in the balance between caldesmon regulated by p21-activated kinases and the Arp2/3 complex govern podosome formation. J Biol Chem 282:8454–8463

Müller-Hermelink HK, Heusermann U, Stutte HJ (1974) Enzyme histochemical observations on the localization and structure of the T cell and B cell regions in the human spleen. Cell Tissue Res 154:167–179

Muñoz-Fernández R, Blanco FJ, Frecha C, Martín F, Kimatrai M, Abadía-Molina AC, García-Pacheco JM, et al. (2006) Follicular dendritic cells are related to bone marrow stromal cell progenitors and to myofibroblasts. J Immunol 177:280–289

Nakayama H, Miyazaki E, Enzan H (1999) Differential expression of high molecular weight caldesmon in colorectal pericryptal fibroblasts and tumour stroma. J Clin Pathol 52:785–786

Ngai PK, Walsh MP (1984) Inhibition of smooth muscle actin-activated myosin Mg2+-ATPase activity by caldesmon. J Biol Chem 259:13656–13659

Nolte MA, Beliën JA, Schadee-Eestermans I, Jansen W, Unger WW, van Rooijen N, Kraal G, et al. (2003) A conduit system distributes chemokines and small blood-borne molecules through the splenic white pulp. J Exp Med 198:505–512

Perez-Montiel MD, Plaza JA, Dominguez-Malagon H, Suster S

(2006) Differential expression of smooth muscle myosin, smooth muscle actin, h-caldesmon, and calponin in the diagnosis of myofibroblastic and smooth muscle lesions of skin and soft tissue. Am J Dermatopathol 28:105–111

Pinkus GS, Warhol MJ, O'Connor EM, Etheridge CL, Fujiwara K (1986) Immunohistochemical localization of smooth muscle myosin in human spleen, lymph node, and other lymphoid tissues. Unique staining patterns in splenic white pulp and sinuses, lymphoid follicles, and certain vasculature, with ultrastructural correlations. Am J Pathol 123:440–453

Qiu X, Montgomery E, Sun B (2008) Inflammatory myofibroblastic tumor and low-grade myofibroblastic sarcoma: a comparative study of clinicopathologic features and further observations on the immunohistochemical profile of myofibroblasts. Hum Pathol 39:846–856

Satoh T, Sakurai E, Tada H, Masuda T (2009) Ontogeny of reticular framework of white pulp and marginal zone in human spleen: immunohistochemical studies of fetal spleens from the 17th to 40th week of gestation. Cell Tissue Res 336:287–297

Satoh T, Takeda R, Oikawa H, Satodate R (1997) Immunohistochemical and structural characteristics of the reticular framework of the white pulp and marginal zone in the human spleen. Anat Rec 249:486–494

Schuler W, Weiler IJ, Schuler A, Phillips RA, Rosenberg N, Mak TW, Kearney JF, et al. (1986) Rearrangement of antigen receptor genes is defective in mice with severe combined immune deficiency. Cell 46:963–972

Sobue K, Sellers JR (1991) Caldesmon, a novel regulatory protein in smooth muscle and nonmuscle actomyosin systems. J Biol Chem 266:12115–12118

Sobue K, Tanaka T, Kanda K, Ashino N, Kakiuchi S (1985) Purification and characterization of caldesmon77: a calmodulin-binding protein that interacts with actin filaments from bovine adrenal medulla. Proc Natl Acad Sci USA 82:5025–5029

Steiniger B, Barth P, Hellinger A (2001) The perifollicular and marginal zones of the human splenic white pulp: do fibroblasts guide lymphocyte immigration? Am J Pathol 159:501–512

Tanaka H, Hataba Y, Saito S, Fukushima O, Miyasaka M (1996) Phenotypic characteristics and significance of reticular meshwork surrounding splenic white pulp of mice. J Electron Microsc (Tokyo) 45:407–416

Toccanier-Pelte MF, Skalli O, Kapanci Y, Gabbiani G (1987) Characterization of stromal cells with myoid features in lymph nodes and spleen in normal and pathologic conditions. Am J Pathol 129:109–118

Tsunoda T, Yamakawa M, Takahashi T (1999) Differential expression of Ca(2+)-binding proteins on follicular dendritic cells in non-neoplastic and neoplastic lymphoid follicles. Am J Pathol 155:805–814

Van den Berg TK, Döpp EA, Brevé JJ, Kraal G, Dijkstra CD (1989) The heterogeneity of the reticulum of rat peripheral lymphoid organs identified by monoclonal antibodies. Eur J Immunol 19: 1747–1756

Veerman AJ, van Ewijk W (1975) White pulp compartments in the spleen of rats and mice. A light and electron microscopic study of lymphoid and non-lymphoid celltypes in T- and B-areas. Cell Tissue Res 156:417–441

Veerman AJ, Vries HD (1976) T- and B-areas in immune reactions. Volume changes in T and B cell compartments of the rat spleen following intravenous administration of a thymus-dependent (SRBC) and a thymus-independent (paratyphoid vaccin-endotoxin) antigen. A histometric study. Z Immunitatsforsch Exp Klin Immunol 151:202–218

Visée S, Soltner C, Rialland X, Machet MC, Loussouarn D, Milinkevitch S, Pasco-Papon A, et al. (2005) Supratentorial primitive neuroectodermal tumours of the brain: multidirectional differentiation does not influence prognosis. A clinicopathological report of 18 patients. Histopathology 46:403–412

Wang CL (2008) Caldesmon and the regulation of cytoskeletal functions. Adv Exp Med Biol 644:250–272

Yokouchi K, Numaguchi Y, Kubota R, Ishii M, Imai H, Murakami R, Ogawa Y, et al. (2006) l-Caldesmon regulates proliferation and migration of vascular smooth muscle cells and inhibits neointimal formation after angioplasty. Arterioscler Thromb Vasc Biol 26:2231–2237

Yoshida K, Matsuura N, Tamahashi N, Takahashi T (1993) Development of antigenic heterogeneity in the splenic meshwork of severe combined immunodeficient (SCID) mice after reconstitution with T and B lymphocytes. Cell Tissue Res 272:1–10

Yoshida K, Tamahashi N, Matsuura N, Takahashi T, Tachibana T (1991) Antigenic heterogeneity of the reticular meshwork in the white pulp of mouse spleen. Cell Tissue Res 266:223–229

The Journal of Histochemistry & Cytochemistry